

Counterfactual Explanation with Multi-Agent Reinforcement Learning for Drug Target Prediction

Tri Minh Nguyen^{1,*}, Thomas P Quinn¹, Thin Nguyen¹ and Truyen Tran¹

¹Applied Artificial Intelligence Institute, Deakin University, Victoria, Australia

*To whom correspondence should be addressed.

Associate Editor: XXXXXXXX

Received on XXXXX; revised on XXXXX; accepted on XXXXX

Abstract

Motivation: Many high-performance DTA models have been proposed, but they are mostly black-box and thus lack human interpretability. Explainable AI (XAI) can make DTA models more trustworthy, and can also enable scientists to distill biological knowledge from the models. Counterfactual explanation is one popular approach to explaining the behaviour of a deep neural network, which works by systematically answering the question "How would the model output change if the inputs were changed in this way?". Most counterfactual explanation methods only operate on single input data. It remains an open problem how to extend counterfactual-based XAI methods to DTA models, which have two inputs, one for drug and one for target, that also happen to be discrete in nature.

Methods We propose a multi-agent reinforcement learning framework, Multi-Agent Counterfactual Drug-target binding Affinity (MACDA), to generate counterfactual explanations for the drug-protein complex. Our proposed framework provides human-interpretable counterfactual instances while optimizing both the input drug and target for counterfactual generation at the same time.

Results: We benchmark the proposed MACDA framework using the Davis dataset and find that our framework produces more parsimonious explanations with no loss in explanation validity, as measured by encoding similarity and QED. We then present a case study involving ABL1 and Nilotinib to demonstrate how MACDA can explain the behaviour of a DTA model in the underlying substructure interaction between inputs in its prediction, revealing mechanisms that align with prior domain knowledge.

Availability: The Python implementation is available at <https://github.com/ngminhtri0394/MACDA>

Contact: minhtri@deakin.edu.au

1 Introduction

Drug-target binding affinity (DTA) prediction is an important step in drug discovery and drug repurposing (Thafar *et al.*, 2019). Many high-performance DTA models have been proposed, but they are mostly black-box and thus lack human interpretability (Öztürk *et al.*, 2018, 2019; Tornig and Altman, 2019; Zheng *et al.*, 2020; Jiang *et al.*, 2020; Nguyen *et al.*, 2020; Tri *et al.*, 2020). This lack of interpretability makes it difficult to use deep learning models to *distill knowledge* about how drugs bind to their targets. Explainable AI methods explain how a model works, and therefore facilitate human knowledge distillation. When applied to DTA prediction, model explanations can produce insights that feedback into the research pipeline and improve our understanding of drug-molecule binding.

Counterfactual explanation is one popular approach to explaining the behaviour of a deep neural network, which works by systematically

answering the question "How would the model output change if the inputs were changed in this way?". Research into this type of explainable AI has mostly focused on image data and tabular data (Vermeire and Martens, 2020; Mothilal *et al.*, 2020; Dhurandhar *et al.*, 2018; Cheng *et al.*, 2020). In the context of the drug-target affinity, counterfactual explanations are not widely used. Instead, explanation methods rely on feature attribution scores and gradients (Preuer *et al.*, 2019; Pope *et al.*, 2019; McCloskey *et al.*, 2019), which may fail to capture high-order interactions between features (Tsang *et al.*, 2018). It remains an open problem of how to produce counter-factual explanations for drug-target affinity models.

There are two key challenges in extending counterfactual explanations to drug-target affinity models. First, the inputs to a DTA model, represented most often as sequences or graphs, are discrete not continuous. Therefore, gradient-based counterfactual generation methods, which operate on the continuous data, cannot be applied. Meanwhile, gradient-free combinatorial methods like *in silico mutagenesis* (Zhou and Troyanskaya, 2015) are computationally expensive to run. Second, DTA models have two distinct

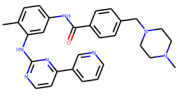
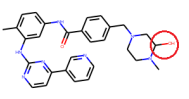
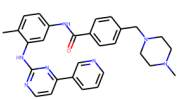
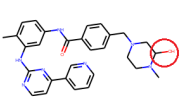
Instance	Drug	Protein	Δ Affinity
Original drug Original protein		...PFWKYY...	0
Counterfactual drug Original protein		...PFWKYY...	High
Original drug Counterfactual protein		...PAWKYY...	High
Counterfactual drug Counterfactual protein		...PAWKYY...	Low

Fig. 1. A summary of the unstable environment problem in drug-target binding affinity counterfactual generation. If the drug or target is fixed, the Δ affinity is high. However, the Δ affinity between counterfactual instance of drug and protein may be low as they are not optimized for new drug/protein.

inputs, the drug and the target. Changes to the drug molecule and protein can both influence the binding affinity, either separately or jointly. Generating counterfactuals for drug and target separately may not lead to an optimal solution (see Fig. 1). On top of that, the substructure interactions between drug functional groups and protein residues are crucial DTA model prediction. However, it is difficult to disentangle and interpret the effect of substructure interaction from the DTA model prediction.

We propose **Multi-Agent Counterfactual Drug-target binding Affinity (MACDA)** framework, which uses multi-agent reinforcement learning (MARL) to solve both challenges. First, MARL solves the challenge of discrete inputs because MARL is naturally designed for *discrete actions*. These actions can serve as a fundamental unit of human-interpretation. In the DTA problem, the adding or removing of bonds and atoms on a drug can be thought of as actions (as can the adding or removing of motifs and residues on a protein). Second, MARL solves the challenge of multiple inputs because the drug and the protein can be represented as different action space inputs within a single model. Third, MACDA isolates the effect of substructure interaction of drug and protein in the model prediction. This allows domain experts to validate the binding mechanism the DTA model used in its prediction.

In contrast to previous work that used reinforcement learning (RL) to facilitate drug synthesis (Zhou et al., 2019), we use RL here to solve a more general problem of explaining the behavior of black-box DTA model in order to understand the biology of drug-protein complex. To this end, we propose the multi-agent RL framework, MACDA, for explaining deep models of drug-target binding affinity. We evaluate the proposed framework on the publicly available Davis dataset, where we observe a stable learning

process and counterfactual explanations that agree with the state-of-the-art method in molecule counterfactual generation.

2 Related works

2.1 Drug-target affinity models

Drug-target binding affinity, measured by a disassociation constant K_d , indicates the strength of the binding force between the target protein and its ligand (drug or inhibitor). Drug-target binding affinity prediction methods can be categorized into two main approaches: structural approach and non-structural approach (Thafar et al., 2019). The structural approach (Meng et al., 1992; Jorgensen et al., 1983; Pullman, 2013; Raha et al., 2007) uses the 3D information of the protein structure and ligand to run a drug-target interaction simulation. The non-structural approach (Nguyen et al., 2020; Öztürk et al., 2018, 2019; Tri et al., 2020) uses other information such as protein sequence, atom valence, hydrophobic, and others to from existing databases to predict the binding affinity. In MACDA, we take the non-structural approach.

2.2 Explaining deep neural networks for DTA

Recently, high accuracy DTA models are often based on deep neural networks, which are mostly black-box. This poses a great question of how to explain the behaviours of the deep models, and distill the explicit knowledge from them. There are two general approaches relevant to the explanation of drug-target affinity models: feature attribution and graph-based methods.

Feature attribution measures the relevance score of the input feature with respect to the predicted affinity score y , either using the gradient (Preuer et al., 2019; Pope et al., 2019) or a surrogate model (Rodríguez-Pérez and Bajorath, 2020). Gradient-based methods take advantage of the derivative of the output with respect to the input. McCloskey et al. (2019) use integrated gradients on graph convolution model trained on the molecular binding synthesis dataset to analyze the binding mechanism. However, gradient-based methods could be misleading or prone to gradient saturation (Ying et al., 2019). Surrogate-based methods generate a surrogate explanatory model g which is interpretable (linear or decision tree) and can approximate the original function f .

Graph-based methods are suitable for DTA because the structure of the drug molecule can be represented naturally with the graph structure. The graph can be explained by subsets of edges and node features which are important for model f prediction of class c . For example, GNNExplainer (Ying et al., 2019) finds a subgraph G' of input graph G , and subfeature X' of input feature X which maximizes the mutual information between $f(G, X)$ and $f(G', X')$, but is argued to not generalize well (Numeroso and Bacciu, 2020). Attention-based graph neural network (Veličković et al., 2018; Shang et al., 2018; Ryu et al., 2018) is a mechanism that can facilitate explanation such as the influence of substructure to the solubility property (Shang et al., 2018), visualizing the importance of neighbor nodes via an attention score. In MACDA, we use a graph-based method.

2.3 Reinforcement learning: Single and Multi-agent

Reinforcement learning (RL) is the process of agent learning to find the optimal action for situations that maximizes the long-term rewards (Sutton and Barto, 2018). For the single agent case, an agent interacts with the environment. At each time step t , the agent observes environment state $s_t \in S$ and chooses an action $a_t \in A$ using its policy $\pi(a_t|s_t)$. By completing the action, the agent receives a reward r_t and changes the environment to the next state s_{t+1} .

There are two main approaches to RL: value-based and policy-based. The value-based methods estimate the value function for each state, where the action is chosen based on the action value. The policy-based methods,

on the other hand, optimize the agent’s policy as a function $\pi(a|s, \theta)$ where θ is the parameter. The two methods can be combined, e.g., both value function and the policy are estimated, as in the celebrated actor-critic methods (Konda and Borkar, 1999; Morimura *et al.*, 2009). In MACDA, we use an actor-critic method.

Multi-agent reinforcement learning (MARL) is the generalization from a single agent to multiple agents that share the same environment. Each agent interacts with the environment and with other agents. The challenge of multi-agent RL is finding the optimal policy for each agent with respect to not only the environment but also to the other agent’s policy. Many approaches solving the multi-agent setting have been proposed, ranging from cooperative communication (Tan, 1993; Fischer *et al.*, 2004) to competitive environment (Littman, 1994; Perez-Liebana *et al.*, 2019). In MACDA, we use cooperative communication.

2.4 Using reinforcement learning for explanations

Instead of assigning a relevance score to the input features of the model, counterfactual explanation finds the simplest perturbed instance with a maximal difference in model prediction outcome (Wachter *et al.*, 2017). The motivation here is that if a small change in part of the input causes a big change in the output, then that part of the input is important.

Reinforcement learning has been used previously to generate counterfactual explanations (Hendricks *et al.*, 2016; Li *et al.*, 2016). Numeroso and Bacciu (2020) generate a counterfactual explanation for a molecule using MEG framework, a multi-objective reinforcement learning, to maximize the prediction model output change while maintaining the similarity between original and counterfactual molecule instances. We use the multi-agent version of the MEG framework as the baseline for our experiments. Compared to multi-agent MEG framework, our proposed MACDA framework uses multi-agent actor-critic approach in which each modification to drug and protein are considered simultaneously.

3 Methods and materials

3.1 Problem definition

A counterfactual explanation is given as a hypothetical statement "If X had been X' , Y would have been Y' " (Pearl *et al.*, 2016; Goyal *et al.*, 2019). The counterfactual explanation X' is an instance which resembles X while leading to a substantially different outcome. To give a counterfactual example of the instance X , we formulate as an optimization problem:

$$\arg \max_X \lambda y_{loss}(Y - Y') + sim(X, X') \quad (1)$$

where $sim(X, X')$ is the similarity between the original instance and counterfactual instance, while λ balances the prediction distance y_{loss} and the similarity.

We extend the hypothetical statement for drug-target pair (D, P) interaction in DTA model \mathcal{F} as "If drug D and protein P interaction had been D' and P' interaction, the predicted affinity $\mathcal{F}(D, P)$ would have been $\mathcal{F}(D', P')$ ".

Given a drug-target pair (D, P) with the predicted binding affinity $\mathcal{F}(D, P)$ in DTA model \mathcal{F} , the task of finding the counterfactual interaction pair (D', P') in \mathcal{F} is the optimizing problem.

$$\arg \max_{D', P'} \lambda_1 y_{loss}(\mathcal{F}(D, P) - \mathcal{F}(D', P')) + \lambda_2 sim(D, D') + \lambda_3 sim(P, P') \quad (2)$$

where $sim(D, D')$ and $sim(P, P')$ measure the similarity between the input instance and counterfactual instance of drug and protein, while λ_1 , λ_2 , and λ_3 are the weight coefficients.

3.2 Counterfactual generation with RL

In this section, we briefly describe the process of generating the counterfactual instance using RL. We choose RL to solve the optimizing the function in Eq. 2 as RL can operate on discrete action space (e.g., to change an atom or amino acid residue). Specifically, we employ Actor-Critic RL (Sutton and Barto, 2018). Unlike Q-learning which tries to evaluate the Q-value of all actions and choose an action with greedy algorithm, ACRL learns to choose the action robustly with policy network π . In ACRL, a Q-value network assists the policy network by updating the policy network parameter θ . The intuition behind the policy network π and Q-value network Q in ACRL is that the policy network is the actor, learning a robust strategy, and the Q-value network is the critic, correcting the actor strategy.

Our ACRL framework consists of two main components: **(a)** the agent and **(b)** the simulated environment with the model \mathcal{F} as its core. The agent choose an **action** and **interacts with the environment**. By **action** we mean that the agent chooses a modified version of the input drug or protein. By **interacts with the environment**, we mean that the model \mathcal{F} receives a modified version of drug and protein, then suggests their simulated binding affinity.

The environment has the model \mathcal{F} as its core to calculate the binding affinity between drug and protein generated by agents. After calculating the affinity, the environment will return the **state** of drug and protein and the **reward** (see Fig. 2). The returned state is a Morgan fingerprint for drug and a protein sequence for target. The reward goal is to optimize the counterfactual function Eq. 2. We will further describe the reward function in Sec. 3.3.3.

The agent handles the counterfactual example generation based on the environment state and reward. In our case, the agent generates a modified version of the input drug and protein state. The ACRL agent has two main components: **(a)** policy network with parameter θ and **(b)** Q-value network with parameters ψ .

The Q-value network $Q_\psi(s, a)$ plays a role as critic, updated using Q loss (see Fig. 2). Given an action-state (s, a) with reward R_t at time step t and action-state (s', a') at time step $t' = t + 1$, the parameter ψ is updated with the Q loss function:

$$\mathcal{L}_Q = R_t + \gamma Q_\psi(s', a') - Q_\psi(s, a) \quad (3)$$

where γ is the discount factor. The policy network π_θ decides which action to take. A policy is the probability of each action being selected. The actor updates the θ parameter of the policy network with the suggestion of critic:

$$\theta \leftarrow \theta + \alpha Q_\psi(s, a) \nabla_\theta \log \pi_\theta(a|s) \quad (4)$$

where α is the learning rate.

3.3 Drug-protein pair counterfactual generation with MARL

We now describe our MARL framework which is the extension from the ACRL framework (in Sec. 3.2) for generating drug-target counterfactuals. MARL is particularly suitable because it works naturally on multiple discrete action spaces. In our setting, the two action spaces correspond to the discrete modifications in the molecule space and protein space, respectively. In particular, we will employ a MARL framework known as Multi-agent Actor-Attention-Critic (MAAC) (Iqbal and Sha, 2019). This framework is flexible, easy to train, and is natural for exploring the joint space of protein-drug complex. MAAC allows separated policies for drug and protein, but with common critics and rewards. It uses the attention mechanism to dynamically select relevant information shared by the other agent, a procedure that resembles the selective binding mechanism often found in the protein-drug complex (Tri *et al.*, 2020).

The framework is illustrated in Fig. 2. There are two agents: one generates counterfactuals for the protein, and the other for the drug. The

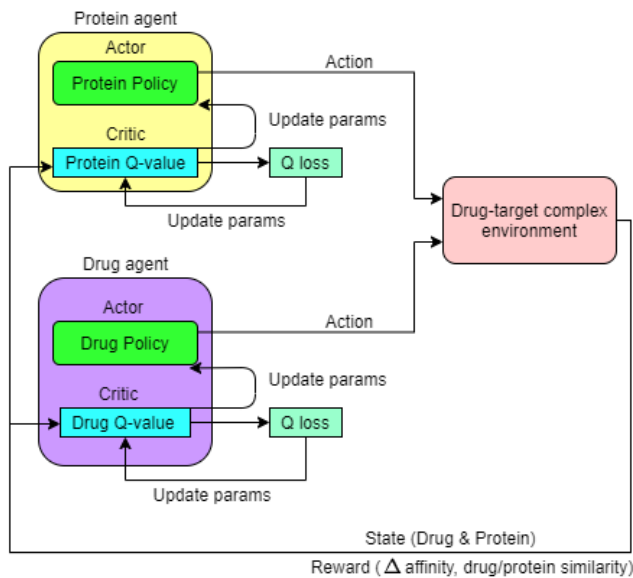


Fig. 2. The overview of MARL framework for drug-target counterfactual generation. Two agents, protein and drug, have their own actor and critic. The actor chooses the action using its policy. Two agents take actions and the drug-target environment returns (a) the new state of drug and protein, and (b) the reward, which is a sum of the prediction change and the protein/drug similarities. Then, the critic calculates its Q value using the reward value. The Q value is used to update the critic network.

two agents work in tandem to produce joint counterfactuals for the protein-drug complex. Each agent has its own Q-value function. Two agents communicate through the reward function described in Eq. 13 and through the Q-value function (Eq. 5).

In what follows, we describe the framework components. In particular, the action space for drug and protein are provided in Sec. 3.3.1 and Sec. 3.3.2. The overall reward is presented in Sec. 3.3.3.

3.3.1 Available drug actions

We adopt the drug molecule generation strategy in Mol-DQN (Zhou *et al.*, 2019). There are three action categories: (a) **Add atom**: Given an admissible set of atoms $\mathcal{E} = \{Atom_1, \dots, Atom_N\}$, one atom $Atom_i$ is inserted into the drug molecule at a time. Then a bond is formed between the newly added atom and a position satisfying the valence constraint. Therefore, given n_p positions satisfying the constraint, there are n_p instances generated. (b) **Add bond**: One or more bond is added up to triple bond between two atoms with free valence. (c) **Remove bond**: One or more bond is removed from the existing bond. If there is no bond between two atoms after removal, then the disconnected atom is removed.

All possible actions are generated and used as action space in the reinforcement learning framework described in Sec. 3.3.3.

3.3.2 Available protein actions

For proteins, there is only one action category: (a) **Replace amino acid residue with alanine**. Alanine is widely used to determine the contribution of protein residues in the protein function or drug-protein binding (Gray *et al.*, 2017). Alanine is chosen as its size is not too large which avoids steric hindrance. In addition, the methyl function group allows it to mimic the secondary structure of the residues it replaces ((Gray *et al.*, 2017)). This process is known as alanine scanning (Gray *et al.*, 2017). For the protein sequence $P = r_i, i \leq l$ where l is protein sequence length, a single residue r_i is replaced with alanine to create a single point alanine mutation. All possible single point mutations are generated and used as the action space.

3.3.3 Multi-agent actor-attention-critic for counterfactual generation

The idea of multi-agent actor-critic is that the Q-value function of agent i is calculated based on the observation of other agents $s = (s_1, \dots, s_N)$:

$$Q_i^{\theta} = f_i(g_i(s_i, a_i), x_i) \quad (5)$$

where f_i and g_i are multi-layer perceptron, x_i is the weighted sum of other agents value:

$$x_i = \sum_{j \neq i} \alpha_{ij} \sigma(Vg_j(s_j, a_j)) \quad (6)$$

where V is the linear transformation, σ is Leaky ReLU, and α_{ij} is the attention score computed as in (Vaswani *et al.*, 2017) by taking g_i, g_j as the inputs. Learning in this actor-critic framework then proceeds for each agent using the framework described in Sec. 3.2.

In our context of protein-drug counterfactual generations, this boils down to using state-action function of drug agent to influence the Q-function of the protein agent and vice versa. In particular, the Eq. 5 and Eq. 6 for drug agent become:

$$Q_d^{\theta} = f_d(g_d(s_d, a_d), x_d) \quad (7)$$

where

$$x_d = \sigma(Vg_p(s_p, a_p)) \quad (8)$$

The Q-value function for protein is calculated in the similar manner.

Multi-objective reward function: Our objective is to find the counterfactual satisfying two constraints: (1) to maximize the change in the predicted binding affinity, and (2) to maximize the similarity between original instance and counterfactual instance.

The Δ affinity between the predicted value of counterfactual drug-protein (D', P') and the predicted value of the original instance (D, P), $\Delta\mathcal{F}(D', P')$, is calculated as:

$$\Delta\mathcal{F}(D', P') = y_{loss}(\mathcal{F}(P', D') - \mathcal{F}(P, D)) \quad (9)$$

Here, we choose y_{loss} to be absolute error.

Our target is identifying the joint importance of drug sub-structures and protein residues using the joint counterfactual. In other words, we identify which parts of the drug and protein interacting in the DTA model. However, the $\Delta\mathcal{F}(D', P')$ only considers the consequences of the total drug-target counterfactual. It does not isolate the effect of the joint counterfactual. The joint drug-target counterfactual $\Delta\mathcal{F}$ affinity change is given as:

$$\Delta_{joint}\mathcal{F}(D', P') = \Delta\mathcal{F}(D', P') - \Delta\mathcal{F}(D', P) - \Delta\mathcal{F}(D, P') \quad (10)$$

where $\Delta\mathcal{F}(D, P')$ and $\Delta\mathcal{F}(D', P)$ are counterfactual target - fixed drug $\Delta\mathcal{F}$ affinity, and vice versa. Simply speaking, the joint drug-target counterfactual $\Delta\mathcal{F}$ affinity shows contribution of perturbing both drug and protein jointly. Interacting drug-substructure and protein residue should change the affinity prediction more than the sum of the individual perturbations. A high $\Delta_{joint}\mathcal{F}(D', P')$ shows that the DTA model factors the drug-substructure and protein residue interaction in its prediction.

As our goal is identifying the interacting drug sub-structure residue pair, we add the sign function to give negative reward when the generated (D', P') pair increases the affinity:

$$\begin{aligned} \Delta_{joint}\mathcal{F}(D', P') &= -\text{sign}(\mathcal{F}(P', D') - \mathcal{F}(P, D)) \times \Delta\mathcal{F}(D', P') \\ &\quad - \Delta\mathcal{F}(D', P) - \Delta\mathcal{F}(D, P') \end{aligned} \quad (11)$$

The similarity is the cosine similarity:

$$d(\mathcal{F}_e(x), \mathcal{F}_e(y)) = \frac{\mathcal{F}_e(x) \cdot \mathcal{F}_e(y)}{\|\mathcal{F}_e(x)\| \|\mathcal{F}_e(y)\|}. \quad (12)$$

where \mathcal{F}_e is the encoded representation of drug or protein in the DTA model. In case the encoded representation is not available, the Tanimoto similarity between two molecule fingerprints and protein sequence similarity can be used as the alternative similarity.

Then the reward function is defined as:

$$\begin{aligned} R(s) &= \alpha_r \Delta_{joint}\mathcal{F}(D', P') + \alpha_p \text{sim}(\mathcal{F}_e(P), \mathcal{F}_e(P')) \\ &\quad + \alpha_d \text{sim}(\mathcal{F}_e(D), \mathcal{F}_e(D')) \end{aligned} \quad (13)$$

where P' and D' are the counterfactual instance of drug D and protein P , α_r , α_d , and α_p are coefficients that balance between the predicted affinity change and the similarity. We add both protein and drug molecule similarity terms to the reward. First, both similarity terms help the model to generate molecules and sequences with minimal change, satisfying one of counterfactual constraints. Second, it works as a communication between two agents where the drug agent searches for a molecule that does not require significant change in protein and vice versa. The first term, $\Delta_{joint}\mathcal{F}(D', P')$, is to meet the model output change constraint. The two similarity terms encourage the similarity between original instance and counterfactual instance.

3.4 Dataset

We evaluate our method MACDA on the Davis dataset (Davis *et al.*, 2011), which contains the drug-target binding affinity of 442 target proteins and 72 drugs. We use pK_D (log kinase dissociation constant) to measure the binding affinity between the target protein and the drug molecule, similar to (Öztürk *et al.*, 2018). The drug-target pairs between Tyrosine-protein kinase ABL1 (Human) and 50 drugs in the training set are chosen to generate counterfactual instances. We choose ABL1 as the crystallized complex of ABL1 with various drugs are available for evaluation.

3.5 Baselines

We compare MACDA with 2 baseline methods. First, for **Joint-List**, we choose the top ten drug and protein counterfactual instances having highest Δ affinity and similarity separately (i.e., top 10 for drugs and top 10 for proteins). Then, the two lists are joined to form drug-protein counterfactual instances. Second, for **MA-MEG**, we extend the molecule counterfactual generation MEG framework (Numeroso and Bacciu, 2020) to the drug-target counterfactual generation task. As the MEG framework only has a single agent handling the optimization for drug molecule, we add another agent handling the protein sequence optimization. The protein agent has the action space described in Sec. 3.3.2. The protein agent calculates and updates its Q-function in the same manner as the drug agent. Two agents work independently to optimize the common reward function (see Eq. (13)).

3.6 Implementation detail

The MACDA framework is implemented in Python using Pytorch. GraphDTA-GCNet (Nguyen *et al.*, 2020) is used as a drug-target binding affinity prediction model because of its simplicity and high performance. GraphDTA-GCNet receives the drug molecule graph and protein sequence

as the inputs. The drug molecule observation in MACDA framework is the drug fingerprint. The protein observation in MACDA framework is the alphabet sequence encoded to integer sequence. The protein sequence length is fixed at 1000 residues. To follow the similarity constraint and alanine scanning procedure (Numeroso and Bacciu, 2021), we set the original drug molecule and protein sequence as the starting point and set the episode length to 1. The balance coefficients $\alpha_r = 1.0$, $\alpha_d = 0.05$, and $\alpha_p = 0.01$ in Eq. 13 are chosen based on our experience.

For each drug-target instance, the top ten counterfactual instances with the highest reward are chosen. The hyperparameters in the experiment are shown in Table 1. The hyperparameters are chosen based on our experience.

Table 1. The hyper-parameters used in the experiments.

Hyper parameters	Value
γ	0.99
Batch size	1024
Policy learning rate	0.001
Critic learning rate	0.001
Number of episode	10000

3.7 Evaluation metrics

Two methods are evaluated using four metrics: average drug encoding similarity, average protein encoding similarity, average Δ_{joint} between the predicted binding affinity of original and counterfactual instance defined in Eq. 10, and drug-likeness (QED) (Bickerton *et al.*, 2012). The similarity score is defined in Eq. (12). The protein, drug similarity, and the Δ affinity evaluate how good the generated counterfactual is. These two metrics follows the counterfactual definition in Sec. 3.1. The Δ affinity metric makes sure the generated counterfactual has substantial change in the affinity. The drug and protein encoding similarity estimates how much the generated drug and protein resemble the original instance. The QED assesses the validity of the drug counterfactual instance (Bickerton *et al.*, 2012). Because we use alanine scanning as the protein single point mutation, the protein sequence does not change significantly. Therefore, the protein sequence validation is not necessary.

4 Results and Discussion

4.1 MACDA produces highly parsimonious explanations

Table 2 shows a comparison of our proposed MACDA framework with baseline methods, where our method exhibits state-of-the-art average Δ_{joint} affinity, drug similarity, protein similarity, and QED. The first baseline, **Joint-List**, simply chooses the top drug and protein counterfactuals, then joins them together. As such, it cannot find an interacting counterfactual pair. Thus, the average Δ_{joint} of the first baseline is negative. The second baseline, **MA-MEG** does better, having an average Δ_{joint} that is above zero, but still underperforms MACDA.

QED measures the drug-likeness of the molecules, providing an estimate of the validity of a generated drug. In a variant to MACDA, called **MACDA-QED**, we incorporate the QED into the reward function to increase the validity of the generated drug counterfactual. As a result, MACDA-QED increases the QED by 13.1% compared to the QED of the original data. As the QED is higher, the drug similarity is also slightly higher. However, as a trade off, the average Δ_{joint} is lower since the QED imposes another constraint on the generated drug distribution. Therefore, the counterfactual drug distribution is closer to the original drug distribution.

The average drug similarity and protein similarity columns show us that the MACDA counterfactuals are very similar to the original drug/protein input. Yet, the changes have a big impact on Δ_{joint} . We consider MACDA explanations to be more parsimonious because small changes in the input can produce big changes in joint affinity prediction.

Table 2. The average Δ_{joint} , drug encoding similarity, target encoding similarity, and QED. MACDA is highly parsimonious in that it can find small changes to the input that produce big changes to the joint predicted affinity.

Method	Avg. Δ_{joint} \uparrow	Avg. Drug Sim. \uparrow	Avg. Protein Sim. \uparrow	QED \uparrow
Original drug/protein	0	1	1	0.4366
Joint-List baseline (Ours)	-0.0085	0.9208	0.9992	0.4051
MA-MEG* (Numeroso and Bacciu, 2020)	0.0178	0.9274	0.9993	0.4086
MACDA (Ours)	0.0254	0.9209	0.9993	0.4056
MACDA-QED (Ours)	0.0224	0.9481	0.9993	0.4586

(*) Our extended version of single-agent MEG framework

4.2 MACDA explains DTA model binding site

We measure the frequency of mutation points in the ABL1 kinase domain over 500 counterfactual instances made from the Davis dataset (see Fig. 3). Top common mutation points are MET.244, LYS.247, VAL.260, GLU.286, LYS.291, and VAL.448. Importantly, most of these are, or in close proximity to, known binding sites of various drugs such as Nilotinib (LYS.247, GLU.286, LYS.291, and MET.318, see Fig. 4), Imatinib (LYS.247, GLU.286, and LYS.291), and Asciminib (VAL.448, see Fig. 5).

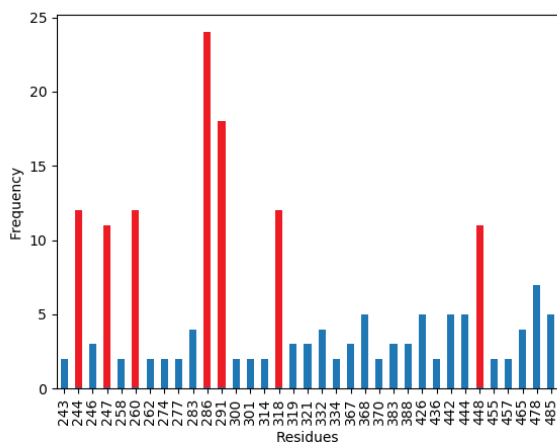


Fig. 3. The mutation point distribution in the kinase domain of ABL1 over 500 counterfactual instances of 50 ABL1-drugs pairs. The top occurrences of alanine replacements are highlighted in red: residues MET.244, LYS.247, VAL.260, GLU.286, LYS.291, and VAL.448 cause the highest change in binding affinity.

4.3 ABL1-Nilotinib study case

We choose Nilotinib for an in-depth case study because the ABL1-Nilotinib has the smallest prediction error in all ABL1-drugs pairs that also have the interaction and crystal structure available for assessment (c.f., PDB 3CS9).

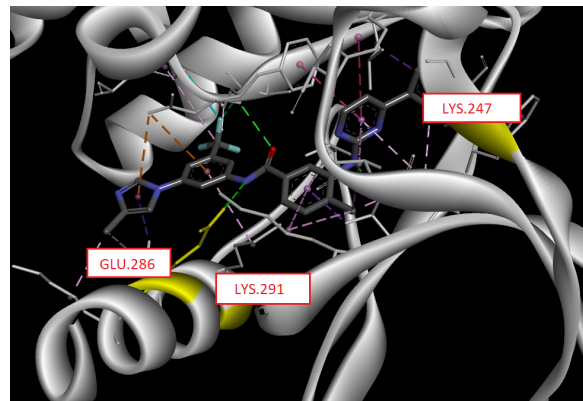


Fig. 4. Visualization of residue LYS.247, GLU.286, and LYS.291 of protein ABL1 in the ABL1-Nilotinib (PDB 3CS9). Note the proximity between Nilotinib and residues LYS.247, GLU.291. Another important residue, GLU.286, is the binding site of ABL1-Nilotinib. Figure best viewed in color.

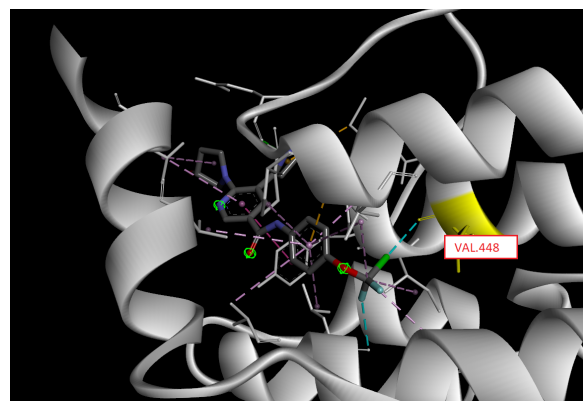


Fig. 5. Visualization of residue VAL.448 of protein ABL1-Asciminib (PDB 5MO4). The residue VAL.448 is the binding site of ABL1-Asciminib. Figure best viewed in color.

Fig. 6 shows the 3 Nilotinib counterfactuals that have the highest Δ_{joint} when interacting with ABL1. In counterfactuals (b) and (c), the (trifluoromethyl)benzenes and residue GLU.286 are modified which leads to high Δ_{joint} . We interpret this to mean that the interaction between the (trifluoromethyl)benzenes and E286 contributes strongly to the DTA model prediction for ABL1-Nilotinib. This also seems to be a biologically plausible binding mechanism. Based on the crystal structure, there is a hydrogen bond between the (trifluoromethyl)benzenes and the GLU.286 (see Fig. 7). In counterfactual (d), it can be suggested that the DTA model also takes into account the interaction between pyrimidine and MET.318 in its prediction.

5 Conclusion

We have proposed a multi-agent reinforcement learning framework named MACDA (Multi-Agent Counterfactual Drug-target binding Affinity) to generate counterfactual explanations for the drug-target binding affinity model. To address the discrete molecule graphs and protein sequences, we use reinforcement learning to generate the counterfactual instances which maximize the change in the binding affinity and the similarity between counterfactual instances and original instances. To address the two-input problem of drug-target binding affinity prediction model, we use multi-agent reinforcement learning. Our multi-agent RL framework consists of a

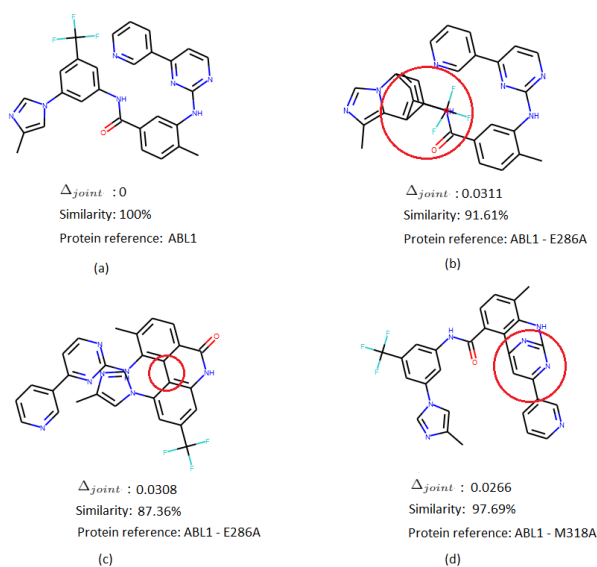


Fig. 6. Panel (a) is the original Nilotinib molecule. Panels (b)-(d) are three high Δ_{joint} counterfactual instances of Nilotinib coupled with counterfactual instances of ABL1 as protein reference. The modification is circled in red. The counterfactual samples explain the interaction between the drug substructures and residues. For example in panel (b), the (trifluoromethyl)benzenes and residue E286 are modified which leads to the highest Δ_{joint} . Therefore, MACDA suggests that the interaction between (trifluoromethyl)benzenes and E286 contributes most to the DTA model decision.

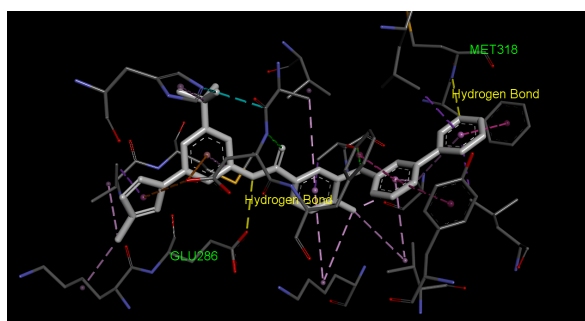


Fig. 7. The hydrogen bond between GLU.286 of ABL1 and the (trifluoromethyl)benzenes group of Nilotinib (PDB 3CS9). Our model suggests cooperative binding between this position which seems plausible given the crystal structure. Figure best viewed in color.

protein agent and a drug molecule agent. Both agents cooperate with each other to optimize the common multi-objective reward. The experiments show that the proposed framework provides a stable learning process and generates the counterfactual instances which maximize the binding affinity change and minimize the joint change in the input.

This work opens opportunities for future research. The counterfactual instances for protein sequences are currently limited to the alanine scanning process which is single point alanine mutation. Furthermore, the binding between drug and target protein does not simply rely on a single residue but on a subset of residues around the binding pocket. Instead of scanning using a single residue, protein sequence motifs could be used. For the drug molecules, the counterfactual instances can be generated at the fragment level instead of the atom level to maintain the drug-likeness of the molecules. These all present open problems whose solutions could further improve joint affinity prediction and explanation parsimony.

References

- Bickerton, G. R. *et al.* (2012). Quantifying the chemical beauty of drugs. *Nature Chemistry*, **4**(2), 90–98.
- Cheng, F. *et al.* (2020). DECE: Decision Explorer with Counterfactual Explanations for Machine Learning Models. *IEEE Transactions on Visualization and Computer Graphics*.
- Davis, M. I. *et al.* (2011). Comprehensive analysis of kinase inhibitor selectivity. *Nature Biotechnology*, **29**(11), 1046–1051.
- Dhurandhar, A. *et al.* (2018). Explanations based on the Missing: Towards Contrastive Explanations with Pertinent Negatives. In *Advances in Neural Information Processing Systems*, pages 592–603.
- Fischer, F. *et al.* (2004). Hierarchical Reinforcement Learning in Communication-Mediated Multiagent Coordination. In *Proceedings of the Third International Joint Conference on Autonomous Agents and Multiagent Systems-Volume 3*, pages 1334–1335.
- Goyal, Y. *et al.* (2019). Counterfactual Visual Explanations. In K. Chaudhuri and R. Salakhutdinov, editors, *Proceedings of the 36th International Conference on Machine Learning*, volume 97 of *Proceedings of Machine Learning Research*, pages 2376–2384. PMLR.
- Gray, V. E. *et al.* (2017). Analysis of Large-Scale Mutagenesis Data To Assess the Impact of Single Amino Acid Substitutions. *Genetics*, **207**(1), 53–61.
- Hendricks, L. A. *et al.* (2016). Generating Visual Explanations. In *European Conference on Computer Vision*, pages 3–19.
- Iqbal, S. and Sha, F. (2019). Actor-Attention-Critic for Multi-Agent Reinforcement Learning. In *International Conference on Machine Learning*, pages 2961–2970.
- Jiang, M. *et al.* (2020). Drug–target affinity prediction using graph neural network and contact maps. *RSC Advances*, **10**(35), 20701–20712.
- Jorgensen, W. L. *et al.* (1983). Comparison of simple potential functions for simulating liquid water. *The Journal of Chemical Physics*, **79**(2), 926–935.
- Konda, V. R. and Borkar, V. S. (1999). Actor-Critic–Type Learning Algorithms for Markov Decision Processes. *SIAM Journal on control and Optimization*, **38**(1), 94–123.
- Li, J. *et al.* (2016). Understanding Neural Networks through Representation Erasure. *arXiv preprint arXiv:1612.08220*.
- Littman, M. L. (1994). Markov games as a framework for multi-agent reinforcement learning. In *Machine Learning Proceedings 1994*, pages 157–163. Elsevier.
- McCloskey, K. *et al.* (2019). Using attribution to decode binding mechanism in neural network models for chemistry. *Proceedings of the National Academy of Sciences*, **116**(24), 11624–11629.
- Meng, E. C. *et al.* (1992). Automated docking with grid-based energy evaluation. *Journal of Computational Chemistry*, **13**(4), 505–524.
- Morimura, T. *et al.* (2009). A Generalized Natural Actor-Critic Algorithm. *Advances in Neural Information Processing Systems*, **22**, 1312–1320.
- Mothilal, R. K. *et al.* (2020). Explaining Machine Learning Classifiers through Diverse Counterfactual Explanations. In *Proceedings of the 2020 Conference on Fairness, Accountability, and Transparency*, pages 607–617.
- Nguyen, T. *et al.* (2020). GraphDTA: Predicting drug-target binding affinity with graph neural networks. *Bioinformatics*.
- Numeroso, D. and Bacciu, D. (2020). Explaining Deep Graph Networks with Molecular Counterfactuals. *Advances in Neural Information Processing Systems, Workshop on Machine Learning for Molecules*.
- Numeroso, D. and Bacciu, D. (2021). MEG: Generating Molecular Counterfactual Explanations for Deep Graph Networks. In *Proceedings of International Joint Conference on Neural Networks*.
- Öztürk, H. *et al.* (2018). DeepDTA: deep drug–target binding affinity prediction. *Bioinformatics*, **34**(17), i821–i829.

- Öztürk, H. et al. (2019). WideDTA: prediction of drug-target binding affinity. *arXiv preprint arXiv:1902.04166*.
- Pearl, J. et al. (2016). *Causal Inference in Statistics: A Primer*. John Wiley & Sons.
- Perez-Liebana, D. et al. (2019). The Multi-Agent Reinforcement Learning in MalmO (MARLO) Competition. *arXiv preprint arXiv:1901.08129*.
- Pope, P. E. et al. (2019). Explainability Methods for Graph Convolutional Neural Networks. In "Proceedings of the IEEE Conference on Computer Vision and Pattern Recognition", pages 10772–10781.
- Preuer, K. et al. (2019). Interpretable Deep Learning in Drug Discovery. In *Explainable AI: Interpreting, Explaining and Visualizing Deep Learning*, pages 331–345. Springer.
- Pullman, A. (2013). *Intermolecular Forces*, volume 14. Springer Science & Business Media.
- Raha, K. et al. (2007). The role of quantum mechanics in structure-based drug design. *Drug Discovery Today*, **12**(17-18), 725–731.
- Rodríguez-Pérez, R. and Bajorath, J. (2020). Interpretation of compound activity predictions from complex machine learning models using local approximations and shapley values. *Journal of Medicinal Chemistry*, **63**(16), 8761–8777.
- Ryu, S. et al. (2018). Deeply learning molecular structure-property relationships using attention-and gate-augmented graph convolutional network. *arXiv preprint arXiv:1805.10988*.
- Shang, C. et al. (2018). Edge Attention-based Multi-Relational Graph Convolutional Networks.
- Sutton, R. S. and Barto, A. G. (2018). *Reinforcement learning: An introduction*. MIT press.
- Tan, M. (1993). Multi-Agent Reinforcement Learning: Independent vs. Cooperative Agents. In *Proceedings of the Tenth International Conference on Machine Learning*, pages 330–337.
- Thafar, M. et al. (2019). Comparison Study of Computational Prediction Tools for Drug-Target Binding Affinities. *Frontiers in Chemistry*, **7**.
- Torng, W. and Altman, R. B. (2019). Graph Convolutional Neural Networks for Predicting Drug-Target Interactions. *Journal of Chemical Information and Modeling*, **59**(10), 4131–4149.
- Tri, N. et al. (2020). GEFA: Early Fusion Approach in Drug-Target Affinity Prediction. *Advances in Neural Information Processing Systems, Workshop on Machine Learning for Structural Biology*.
- Tsang, M. et al. (2018). Neural Interaction Transparency (NIT): Disentangling Learned Interactions for Improved Interpretability. In S. Bengio, H. Wallach, H. Larochelle, K. Grauman, N. Cesa-Bianchi, and R. Garnett, editors, *Advances in Neural Information Processing Systems 31*, pages 5804–5813. Curran Associates, Inc.
- Vaswani, A. et al. (2017). Attention is all you need. In *Advances in Neural Information Processing Systems*, pages 5998–6008.
- Veličković, P. et al. (2018). Graph Attention Networks. *International Conference on Learning Representations*.
- Vermeire, T. and Martens, D. (2020). Explainable Image Classification with Evidence Counterfactual. *arXiv preprint arXiv:2004.07511*.
- Wachter, S. et al. (2017). Counterfactual explanations without opening the black box: Automated decisions and the GDPR. *Harvard Journal of Law & Technology*, **31**, 841.
- Ying, R. et al. (2019). GNNExplainer: Generating Explanations for Graph Neural Networks. *Advances in Neural Information Processing Systems*, **32**, 9240.
- Zheng, S. et al. (2020). Predicting drug-protein interaction using quasi-visual question answering system. *Nature Machine Intelligence*, **2**(2), 134–140.
- Zhou, J. and Troyanskaya, O. G. (2015). Predicting effects of noncoding variants with deep learning-based sequence model. *Nature Methods*, **12**(10), 931–934.
- Zhou, Z. et al. (2019). Optimization of Molecules via Deep Reinforcement Learning. *Scientific Reports*, **9**(1), 1–10.